RESEARCH ARTICLE | JANUARY 29 2024

Cathodoluminescence investigation of defect states in nand p-type AIN [REE]

Special Collection: (Ultra)Wide-bandgap Semiconductors for Extreme Environment Electronics

Christopher M. Matthews ^⑤ ; Habib Ahmad ^⑥ ; Kamal Hussain ^⑥ ; M. V. S. Chandrashekhar ^⑥ ; Asif Khan ^⑥ ; W. Alan Doolittle [☑] ^⑥



Appl. Phys. Lett. 124, 052102 (2024) https://doi.org/10.1063/5.0183178





CrossMark





Cathodoluminescence investigation of defect states in n- and p-type AIN

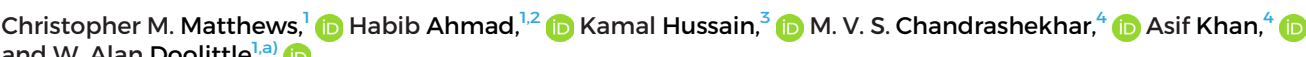
Cite as: Appl. Phys. Lett. **124**, 052102 (2024); doi: 10.1063/5.0183178 Submitted: 21 October 2023 · Accepted: 10 January 2024 · Published Online: 29 January 2024

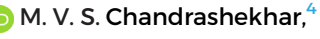






and W. Alan Doolittle^{1,a)} (b)







AFFILIATIONS

- Department of Electrical and Computer Engineering, Georgia Institute of Technology, Atlanta, Georgia 30332, USA
- ²Center for Advanced Electronics and Photovoltaic Engineering, International Islamic University Islamabad, Islamabad, Pakistan
- ³Department of Chemistry and Biochemistry, University of South Carolina, Columbia, South Carolina 29208, USA

Note: This paper is part of the APL Special Collection on (Ultra)Wide-bandgap Semiconductors for Extreme Environment Electronics.

^{a)}Author to whom correspondence should be addressed: alan.doolittle@ece.gatech.edu

ABSTRACT

State-of-the-art semiconducting aluminum nitride (AlN) films were characterized by cathodoluminescence (CL) spectroscopy in the range of 200-500 nm in an attempt to identify the energy levels within the bandgap and their associated defects. Near-band edge emission (around 206 nm) and high-intensity peaks centered in the near UV range (around 325 nm) are observed for both n- and p-type AlN films. The near UV peaks are potentially associated with oxygen contamination in the films. The p-type AlN films contain at least two unidentified peaks above 400 nm. Assuming that the dopant concentration is independent of compensation (i.e., in the perfect doping limit), three effective donor states are found from Fermi-Dirac statistics for Si-doped AlN, at ~0.035, ~0.05, and ~0.11 eV. Similarly, a single effective acceptor energy of ~0.03-0.05 eV (depending on the degeneracy factory considered) was found for Be doped AlN. CL investigation of doped AlN films supports claims that AlN may be a promising optoelectronic material, but also points to contaminant mitigation and defect theory as major areas for future study.

Published under an exclusive license by AIP Publishing. https://doi.org/10.1063/5.0183178

Aluminum nitride (AlN) is a promising candidate for a wide range of applications such as high-power devices for grid scale electronics and electric vehicles, and for ultraviolet (UV) emitters for sterilization and lithography, which are unmet by current materials. Among other wide- and extreme bandgap materials [i.e., gallium nitride (GaN), silicon carbide (SiC), gallium oxide (Ga2O3), and diamond], AlN has a comprehensive set of promising material properties for these applications—namely, a direct bandgap of 6.1 eV, high critical electric field, high thermal conductivity, and compatibility with the established III-nitride infrastructure. 1-6 However, AlN doping, which is required to utilize AlN for these applications, is still an immature topic and requires further investigation.

Silicon-doped AlN was first reported as a natural extension of GaN doping, but early reports of electron concentrations were limited to less than 10¹⁶ cm⁻³. N-AlN with an electron concentration exceeding 10¹⁷ cm⁻³ was reported, but this result appears to have never been repeated and could be complicated by interface conduction between

the film and substrate. Research into doped AlN dwindled in the years that followed. During this time, p-type AlN was never reported and was generally regarded as challenging, if not unrealistic. Due to the limited doping successes, AlN was effectively relegated to being an insulator, rather than living up to its otherwise promising semiconducting properties.

Research into doped AlGaN has since served as a useful tool to understand the challenges associated with AlN doping while simultaneously pushing toward higher bandgap semiconductor materials. Si, Ge, and Mg dopant atoms have been shown to undergo a critical transition as Al-content increases in AlGaN grown by traditional methods, 9,10 which limits carrier concentrations to below the levels needed to realize AlN-based semiconductor devices.

Recently, substantial p- and n-type bulk doping was achieved in AlN:Be and AlN:Si films¹¹⁻¹³ and led to the first demonstration of a homojunction AlN diode. 12 These results represent a significant improvement in achievable carrier concentrations in AlN, with hole

Department of Electrical Engineering, University of South Carolina, Columbia, South Carolina 29208, USA

and electron concentrations of $\sim 4.4 \times 10^{18}$ and $\sim 6 \times 10^{18}$ cm⁻³, orders of magnitude higher than the previous state of the art. 8,11,12,14 In contrast to these results, theoretical investigations into doping AlN have concluded that Be and Si are unlikely to be effective dopants for AlN. Be is expected to occupy deep states in the bandgap, ¹⁵ but these reports do not typically account for impurity band formation.¹³ Additionally, Si is typically expected to be compensated by various defects related to aluminum vacancies and DX-center formation. Despite outperforming theoretical predictions for doping, these early results are plagued with low dopant activation efficiencies. This will later be shown to be consistent with degenerate doping statistics but could also be a result of compensation issues, presumably from undesirable impurities like oxygen, which are gettered by the highly reactive Al- and Be-rich surfaces used to facilitate growth. In this Letter, doped AlN films were characterized by cathodoluminescence (CL) spectroscopy in an attempt to better understand the energy levels within the AlN bandgap.

The films were grown by metal-modulated epitaxy (MME) 16 in a Riber 32 MBE chamber on HVPE AlN-on-sapphire templates. Two-inch wafers were backside metalized with Ta to ensure uniform temperatures during growth and then diced into $1 \times 1 \, \mathrm{cm}^2$ samples for growth. Prior to loading into vacuum, the samples were cleaned with a piranha solution and dipped in dilute HF to remove organic contaminants and some surface oxides, respectively. Al, Be, and Si fluxes were supplied from standard effusion cells, while active nitrogen was generated using a Veeco UNI-bulb radio frequency plasma source. 500 nm thick AlN:Si films were grown directly on the HVPE templates, while 150 nm thick AlN:Be films were grown on 300 nm thick unintentionally doped AlN buffer layers. More detailed sample preparation and growth conditions can be found in Refs. 11 and 12. CL spectra were obtained using a scanning electron microscope equipped with a parabolic mirror spectrometer.

As shown in Table I, the AlN:Si films were doped from $[Si] = 5 \times 10^{17}$ to 7×10^{19} cm⁻³ resulting in electron concentrations ranging from below 9×10^{17} to 6×10^{18} cm⁻³, while the AlN:Be films (Table II) were doped from $[Be] = 7 \times 10^{18}$ to 4×10^{19} cm⁻³ with hole concentrations from 1.1×10^{18} to 3.1×10^{18} cm⁻³. The moderate dopant activation efficiencies may be a result of defect compensation, possibly by the deep states observed here in CL or by others that are not optically active, but they may also be explained by considering degenerate doping. Due to the complex nature of modeling the density of states in an impurity band, the precise factors dictating the doping efficiency cannot be identified here. However, some insight can be gleaned by treating the impurity bands as isolated, effective donor or acceptor energies, E_D or E_A , as has previously been extracted from Hall measurements for GaN containing impurity bands. ¹⁷ We emphasize that

TABLE I. Si-doped AIN information.

Sample ID	[Si] (cm ⁻³)	[e ⁻] (cm ⁻³)	E_{c} - E_{f} (eV)	E _c -E _D (eV)
N4591	5×10^{17}	unmeas.	N/A	N/A
N4592	3×10^{18}	9×10^{17}	0.048	0.052
N4595	8×10^{18}	5×10^{17}	0.064	0.116
N4596	3×10^{19}	1×10^{18}	0.045	0.113
N4597	7×10^{19}	6×10^{18}	-0.007	0.036

TABLE II. Be-doped AIN information.

Sample ID	[Be] (cm ⁻³)	$[h^{+}] (cm^{-3})$	$E_{f}E_{v}$ (eV)	E_A - E_v (eV)
N4491 N4492	4×10^{19} 7×10^{18}	3.1×10^{18} 1.1×10^{18}	0.000 0.030	0.028 0.036

these effective dopant energies are not real and only account for the complex ionization effects of the impurity band occupancy (ionization). In this simplified case, as the Fermi energy moves above the donor energy or as it moves below the acceptor energy, significant loss of dopant ionization results, sharply reducing ionization efficiency.

The expected effective donor and acceptor levels (E_D and E_A) in these films can be calculated by using Fermi–Dirac statistics in the charge neutrality formula in Eq. (1). N_D and N_A represent the concentration of donors and acceptors in cm⁻³, respectively. N_c and N_v represent the effective density of states in the conduction and valence bands in cm⁻³, respectively. The Fermi level is E_b and E_c and E_v represent the conduction and valence band energies, respectively. The spin degeneracy factors of donors and acceptors are given as g_D and g_A , and kT represents thermal energy, which is equal to $\sim 0.0259 \, eV$ at room temperature. $F_{1/2}$ is the Fermi–Dirac integral of order $^{1}/_{2}$ and accounts for the degenerate doping statistics,

$$N_{\nu} \frac{2}{\sqrt{\pi}} F_{1/2} \left(\frac{E_{\nu} - E_{f}}{kT} \right) - \frac{N_{A}}{1 + g_{A} \exp\left((E_{A} - E_{f})/kT \right)}$$

$$= N_{c} \frac{2}{\sqrt{\pi}} F_{1/2} \left(\frac{E_{f} - E_{c}}{kT} \right) - \frac{N_{D}}{1 + g_{D} \exp\left((E_{f} - E_{D})/kT \right)}. \quad (1)$$

Assuming that the left-hand side of Eq. (1) is negligible for n-type AlN, and that the right-hand side is negligible for p-type AlN, ED and E_A can be calculated by iterating over different values of E_f. The result of this calculation for each sample is also shown in Tables I and II. It is evident that each sample in this study is degenerately doped, with the Fermi level lying within 3 kT of the conduction and valence band for the n- and p-type films, respectively. The donor level is predicted to have at least three energies at \sim 35, \sim 50, and \sim 115 meV below the conduction band assuming $g_D = 2$. These energies give expected emission wavelengths of \sim 204, \sim 205, and \sim 207 nm, respectively, so they are expected to be indistinguishable from near-band edge (NBE) peaks in these films. In prior studies, it was found that the effective acceptor energy decreased from \sim 110 to \sim 51 meV as the activated dopant concentration increased within the degenerate regime.¹⁷ Discounting N4592, which has an ionized donor concentration below the critical concentration for impurity band formation, 13 there is a similar general reduction in the donor effective activation energy with increasing electron concentration. Other possible origins of these levels are unknown, as the effective donor levels are not correlated with Si concentration, chamber growth history, or any other conditions that were monitored during the growth of these films.

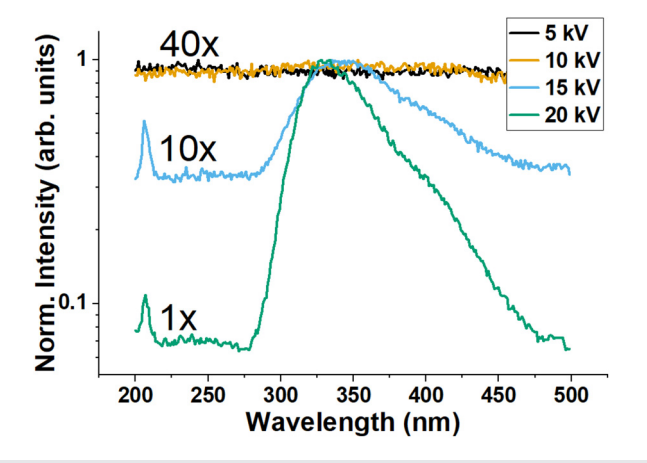
The p-type samples are found to have effective acceptor levels around 30 meV above the valence band when assuming $g_A = 4$ (due to heavy and light hole bands dominating hole conduction), which agrees with the acceptor activation energy extracted from temperature-dependent Hall measurements on Be-doped AlN.¹¹ The expected emission wavelength of these films is ~ 205 nm, and it is also expected

to be indistinguishable from the NBE peak. If $g_A = 2$, which could result from the expected dominance of the crystal-field split-off band for hole conduction in AlN, ¹³ then the effective acceptor level shifts to a slightly higher value of \sim 50 meV above the valence band.

Signal strength is always a concern in CL, and for thin films, the acquisition of a detectable signal must be balanced against a penetration depth that can go beyond the film thickness. CL of each doped AlN film was performed at an excitation energy of 5, 10, 15, and 20 kV corresponding to a range of penetration depths from approximately 200 nm to 2.3 μ m. The CL at each beam energy is shown for sample N4595 in Fig. 1. Luminescence peaks were not observed until the excitation energy was above 10 kV, which indicates that luminescence in AlN is subject to parasitic recombination from the surface. 19 Thus, CL was necessarily collected from both the film and the template in order to get a measurable spectrum, and 15 kV was chosen as the excitation energy for this report to minimize the contribution from the HVPE AlN template layer. Each CL spectrum presented throughout the remainder of this Letter includes a substrate reference in order to distinguish which features come from the film and which come from the substrate.

Figure 2 shows the CL spectra of n-type AlN films. For most films, the spectrum is dominated by a near UV (NUV) peak around 330–340 nm, and the intensity of this peak increases with both increasing Si and electron concentrations. The CL spectra also show a relatively low intensity peak consistently at 206 nm, which is identified as near-band edge (NBE) emission. Finally, a broad, low-intensity peak appears near 224 nm in the CL spectrum for the higher doped AlN films but appears to blend into the noise background as doping is decreased.

The NUV peaks correspond to energies between 3.6 and $3.8 \,\mathrm{eV}$, which are close to the values that have previously been attributed to aluminum vacancy-oxygen defect complexes in AlN. 20,21 These films were grown under conditions that are expected to minimize the presence of both V_{Al} and oxygen in undoped films. 13 However, theory predicts that increasing Si content lowers the formation energy of V_{Al} in AlN, 22 which could lead to a substantial number of V_{Al} -based defect complexes despite the growth conditions. Thus, the NUV peaks in the n-type AlN films reported here can likely be attributed to aluminum



 $\textbf{FIG. 1.} \ \ \text{Representative cathodoluminescence spectra as a function of excitation energy for an n-type AIN:Si film.}$

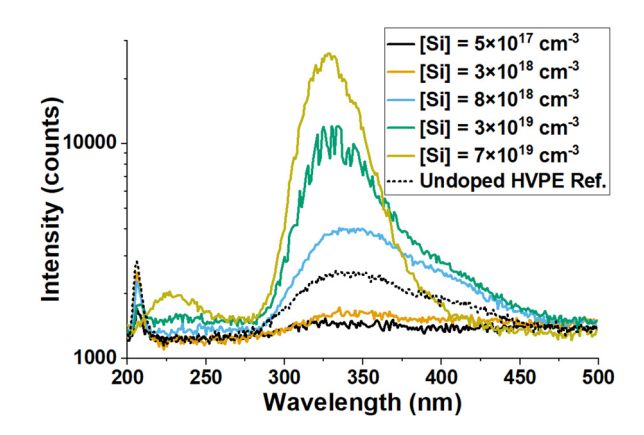


FIG. 2. Cathodoluminescence spectra for n-type AIN:Si films.

vacancy-oxygen defects in the films. Furthermore, given the direct correlation of the NUV peak intensity with the Si doping, it is likely that the source of the oxygen in these films is related to the hot Si effusion cell. CO and CO_2 are known to evolve from hot effusion cells, and the contamination levels of these species depend strongly on operation temperature. Given these Si effusion cells were operated at near their thermal limits, future effort may be required to find alternative means of introducing silicon dopants without compensating contaminants.

The presence of NBE emission in Si-doped AlN indicates relatively high-quality material, and the slight redshift (of ~80 meV) from the theoretical AlN peak may further confirm the n-type nature of these films. Alternatively, one report gives the bandgap of AlN as 6.026 eV at room temperature, 23 which matches the reported NBE emission. In either case, the presence of the NBE peak suggests future optoelectronic devices are practical for MME-grown AlN. For the samples that have measurable conduction (i.e., excluding N4591, or the sample with a Si concentration of $5 \times 10^{17} \, \text{cm}^{-3}$), the NBE emission decreases with increasing Si content. Since the oxygen concentration and the intensity of the associated NUV CL emission are also correlated with Si-doping, it is a reasonable assumption that NBE intensity is reduced as a result of recombination in either oxygen- or siliconrelated sites. The broad 224 nm peak that appears in the film with the highest Si concentration represents a distributed range of states in the bandgap centered approximately 560 meV below the conduction band edge. This is deeper and more distributed in energy than theory suggests for the Si-DX center. The carrier activation efficiency initially drops as dopant concentration increases, but then increases between the second highest and highest doped samples. The ratio of the NUV peak intensity to the intensity at 224 nm increases throughout the full range of Si doping and does not seem to be correlated with the carrier activation efficiency (or compensation). This indicates that the broad peak at 224 nm requires further theoretical investigation.

The CL spectra for p-type AlN films are shown in Fig. 3. Similar to the n-type films, these spectra are dominated by deep level emission, with both AlN:Be films showing high-intensity peaks around 320–330 nm, near the dominant NUV peaks in the AlN:Si films. Interestingly, the intensity of these peaks is inversely proportional to the Be and hole concentration of the films, opposite to the trend observed for the n-type AlN. If this peak is indeed oxygen, its presence may suggest that Be forms defect complexes with O at high

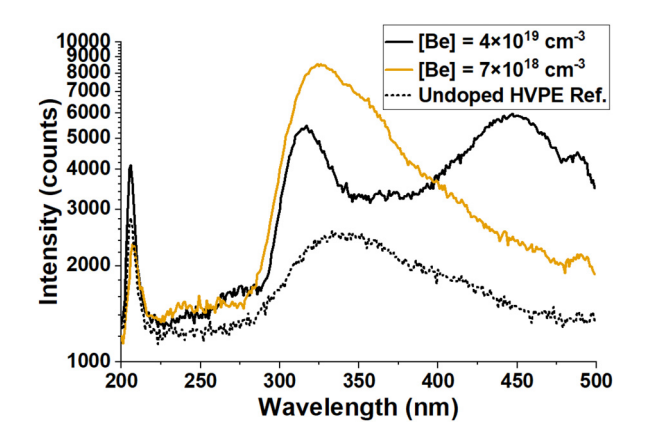


FIG. 3. Cathodoluminescence spectra for p-type AIN:Be films.

concentrations, possibly explaining the chamber-history-dependent variations in hole concentrations. ¹¹ If true, then the Be-O complexes would either (1) have a different yet-to-be-determined CL signature (possibly the deeper 450 nm emission) or (2) be optically inactive.

These films also exhibit NBE emission, but with a direct relationship between doping and peak intensity. The NBE peak intensities for all of the n- and p-type AlN films are all within the same order of magnitude (mid 10³ counts). The highest doped p-type AlN film shows a unique, broad, low-energy emission peak near 450 nm, while both p-type films show an additional broad peak near 490 nm. Finally, a slight increase in the CL intensity is observed between the NBE peak and the dominant NUV peaks for both AlN:Be films, especially when compared to the undoped template, which indicates that there may be broad, low-intensity peaks buried beneath the brighter peaks at longer wavelengths and at wavelengths between the NUV and ~450 nm peaks. Future theoretical work is needed before the defects, which cause these peaks can be definitively identified.

In conclusion, relatively strong near-band edge emission has been observed for both n- and p-type AlN films grown by MME. The consistent presence and similar intensity of these NBE peaks indicated future promise for AlN-based optoelectronics. In both n- and p-type doped AlN films, high-intensity peaks centered in the near UV range suggest that oxygen contamination is a major concern as also seen in the literature for HVPE- and MOCVD-grown AlN. Because degenerate Fermi-Dirac statistics can account for the moderate activation efficiencies, we cannot definitively prove these features are related to compensation. However, future work reducing oxygen concentrations may enable even higher carrier concentrations than those obtained in these films, especially for Si-doped AlN. The CL spectra of Be-doped AlN films contain at least two unidentified features above 400 nm, which could be related to Be defect complexes, but require further theoretical work before they can be definitively identified. CL investigation of doped AlN films supports claims that AlN may be a promising optoelectronic material, but also points to contaminant mitigation as a major area for future study.

This work was supported by the Office of Naval Research (ONR) Multidisciplinary University Research Initiatives (MURI) Program entitled, "Leveraging a New Theoretical Paradigm to

Enhance Interfacial Thermal Transport In Wide Bandgap Power Electronics" under Award No. N00014-17-S-F006 administered by Dr. Mark Spector and Capt. Lynn Petersen. This work was also in part supported by the Air Force Office of Scientific Research under Award No. FA9550-21-1-0318 administered by Dr. Ali Sayir and the Office of Naval Research under Award No. N00014-23-1-2013 administered by Capt. Lynn Petersen.

AUTHOR DECLARATIONS Conflict of Interest

The authors have no conflicts to disclose.

Author Contributions

Christopher M. Matthews: Conceptualization (equal); Data curation (equal); Formal analysis (equal); Investigation (equal); Validation (equal); Visualization (equal); Writing - original draft (equal); Writing - review & editing (equal). Habib Ahmad: Investigation (equal); Validation (equal). Kamal Hussain: Investigation (equal); Validation (supporting). M. V. S. Chandrashekhar: Funding acquisition (equal); Investigation (equal); Resources (equal); Supervision (equal); Validation (equal). Asif Khan: Funding acquisition (equal); Resources (equal); Supervision (equal). William Alan Doolittle: Conceptualization (equal); Data curation (equal); Formal analysis (equal); Funding acquisition (equal); Project administration (equal); Resources (equal); Supervision (equal); Visualization (equal); Writing - review & editing (equal).

DATA AVAILABILITY

The data that support the findings of this study are available from the corresponding author upon reasonable request.

REFERENCES

¹J. Y. Tsao, S. Chowdhury, M. A. Hollis, D. Jena, N. M. Johnson, K. A. Jones, R. J. Kaplar, S. Rajan, C. G. Van de Walle, E. Bellotti, C. L. Chua, R. Collazo, M. E. Coltrin, J. A. Cooper, K. R. Evans, S. Graham, T. A. Grotjohn, E. R. Heller, M. Higashiwaki, M. S. Islam, P. W. Juodawlkis, M. A. Khan, A. D. Koehler, J. H. Leach, U. K. Mishra, R. J. Nemanich, R. C. N. Pilawa-Podgurski, J. B. Shealy, Z. Sitar, M. J. Tadjer, A. F. Witulski, M. Wraback, and J. A. Simmons, "Ultrawide-bandgap semiconductors: Research opportunities and challenges," Adv. Elect. Mater. 4(1), 1600501 (2018).

²W. M. Yim, E. J. Stofko, P. J. Zanzucchi, J. I. Pankove, M. Ettenberg, and S. L. Gilbert, "Epitaxially grown AlN and its optical band gap," J. Appl. Phys. 44(1), 292–296 (1973).

³Y. R. Koh, Z. Cheng, A. Mamun, M. S. Bin Hoque, Z. Liu, T. Bai, K. Hussain, M. E. Liao, R. Li, J. T. Gaskins, A. Giri, J. Tomko, J. L. Braun, M. Gaevski, E. Lee, L. Yates, M. S. Goorsky, T. Luo, A. Khan, S. Graham, and P. E. Hopkins, "Bulk-like intrinsic phonon thermal conductivity of micrometer-thick AlN films," ACS Appl. Mater. Interfaces 12(26), 29443–29450 (2020).

⁴M. S. B. Hoque, Y. R. Koh, J. L. Braun, A. Mamun, Z. Liu, K. Huynh, M. E. Liao, K. Hussain, Z. Cheng, E. R. Hoglund, D. H. Olson, J. A. Tomko, K. Aryana, R. Galib, J. T. Gaskins, M. M. M. Elahi, Z. C. Leseman, J. M. Howe, T. Luo, S. Graham, M. S. Goorsky, A. Khan, and P. E. Hopkins, "High in-plane thermal conductivity of aluminum nitride thin films," ACS Nano 15(6), 9588–9599 (2021).

⁵M. A. Khan, M. Shatalov, H. P. Maruska, H. M. Wang, and E. Kuokstis, "III–Nitride UV devices," Jpn. J. Appl. Phys., Part 1 44(10R), 7191 (2005).

⁶M. Feneberg, R. A. R. Leute, B. Neuschl, K. Thonke, and M. Bickermann, "High-excitation and high-resolution photoluminescence spectra of bulk AlN," Phys. Rev. B **82**(7), 075208 (2010).

- ⁷Y. Taniyasu, M. Kasu, and T. Makimoto, "An aluminium nitride light-emitting diode with a wavelength of 210 nanometres," Nature **441**(7091), 325–328 (2006).
- ⁸T. Ive, O. Brandt, H. Kostial, K. J. Friedland, L. Däweritz, and K. H. Ploog, "Controlled n-type doping of AlN:Si films grown on 6H-SiC(0001) by plasmaassisted molecular beam epitaxy," Appl. Phys. Lett. 86(2), 024106 (2005).
- ⁹J. S. Harris, J. N. Baker, B. E. Gaddy, I. Bryan, Z. Bryan, K. J. Mirrielees, P. Reddy, R. Collazo, Z. Sitar, and D. L. Irving, "On compensation in Si-doped AlN," Appl. Phys. Lett. 112(15), 152101 (2018).
- ¹⁰S. Washiyama, K. J. Mirrielees, P. Bagheri, J. N. Baker, J.-H. Kim, Q. Guo, R. Kirste, Y. Guan, M. H. Breckenridge, A. J. Klump, P. Reddy, S. Mita, D. L. Irving, R. Collazo, and Z. Sitar, "Self-compensation in heavily Ge doped AlGaN: A comparison to Si doping," Appl. Phys. Lett. 118(4), 042102 (2021).
- ¹¹H. Ahmad, J. Lindemuth, Z. Engel, C. M. Matthews, T. M. McCrone, and W. A. Doolittle, "Substantial P-type conductivity of AlN achieved via beryllium doping," Adv. Mater. 33(42), 2104497 (2021).
- ¹²H. Ahmad, Z. Engel, C. M. Matthews, S. Lee, and W. A. Doolittle, "Realization of homojunction PN AlN diodes," J. Appl. Phys. 131(17), 175701 (2022).
- ¹³W. A. Doolittle, C. M. Matthews, H. Ahmad, K. Motoki, S. Lee, A. Ghosh, E. N. Marshall, A. L. Tang, P. Manocha, and P. D. Yoder, "Prospectives for AlN electronics and optoelectronics and the important role of alternative synthesis," Appl. Phys. Lett. 123(7), 070501 (2023).
- 14 M. L. Nakarmi, K. H. Kim, K. Zhu, J. Y. Lin, and H. X. Jiang, "Transport properties of highly conductive n-type Al-rich $Al_xGa_{1-x}N(x\geqslant 0.7),$ " Appl. Phys. Lett. $85(17),\,3769-3771$ (2004).

- 15Y. Zhang, W. Liu, and H. Niu, "Native defect properties and p-type doping efficiency in group-IIA doped wurtzite AlN," Phys. Rev. B 77(3), 035201 (2008).
- ¹⁶H. Ahmad, K. Motoki, E. A. Clinton, C. M. Matthews, Z. Engel, and W. A. Doolittle, "Comprehensive analysis of metal modulated epitaxial GaN," ACS Appl. Mater. Interfaces 12(33), 37693–37712 (2020).
- ¹⁷B. P. Gunning, C. A. M. Fabien, J. J. Merola, E. A. Clinton, W. A. Doolittle, S. Wang, A. M. Fischer, and F. A. Ponce, "Comprehensive study of the electronic and optical behavior of highly degenerate p-type Mg-doped GaN and AlGaN," J. Appl. Phys. 117(4), 045710 (2015).
- 18 T. E. Everhart and P. H. Hoff, "Determination of kilovolt electron energy dissipation vs penetration distance in solid materials," J. Appl. Phys. 42(13), 5837–5846 (1971)
- ¹⁹B. L. Abrams and P. H. Holloway, "Role of the surface in luminescent processes," Chem. Rev. 104(12), 5783–5802 (2004).
- 20 Q. Yan, A. Janotti, M. Scheffler, and C. G. Van de Walle, "Origins of optical absorption and emission lines in AlN," Appl. Phys. Lett. 105(11), 111104 (2014)
- ²¹J. Hyun Kim, P. Bagheri, R. Kirste, P. Reddy, R. Collazo, and Z. Sitar, "Tracking of point defects in the full compositional range of AlGaN via photoluminescence spectroscopy," Phys. Status Solidi A 220(8), 2200390 (2023).
- 22C. Stampfl and C. G. Van de Walle, "Doping of Al_xGa_{1-x}N," Appl. Phys. Lett. 72(4), 459-461 (1998).
- ²³Q. Guo and A. Yoshida, "Temperature dependence of band gap change in InN and AlN," Jpn. J. Appl. Phys., 33(5R), 2453 (1994).